Supplementary materials

A highly durable zinc-air battery from directly integrated $Fe_xNC@NiFe(OH)_x$ bifunctional catalyst

Hao Luo,[a] Yang Li,[b] Wenchao Wang,[a] Tao Zhou,[a] Congxiao Shang [a] and Zhengxiao Guo*[a]

[a]Department of Chemistry, The University of Hong Kong, Hong Kong SAR, China
[b]Department of Mechanical and Aerospace Engineering, The Hong Kong University of Science and Technology, Clear Water Bay, Hong Kong SAR, China

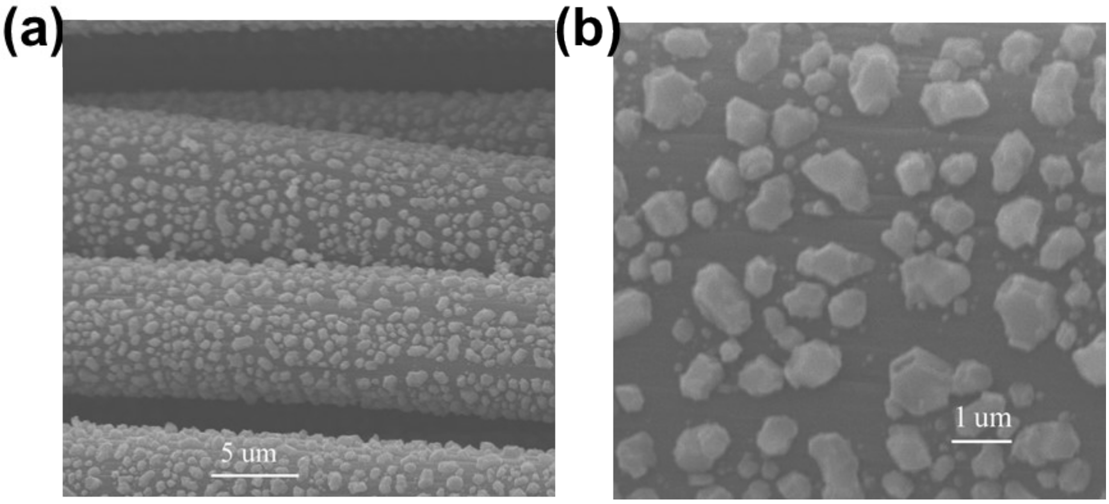

Fig. S1 (a, b) SEM images of $FeFe(CN)_6$ particles on carbon cloth.

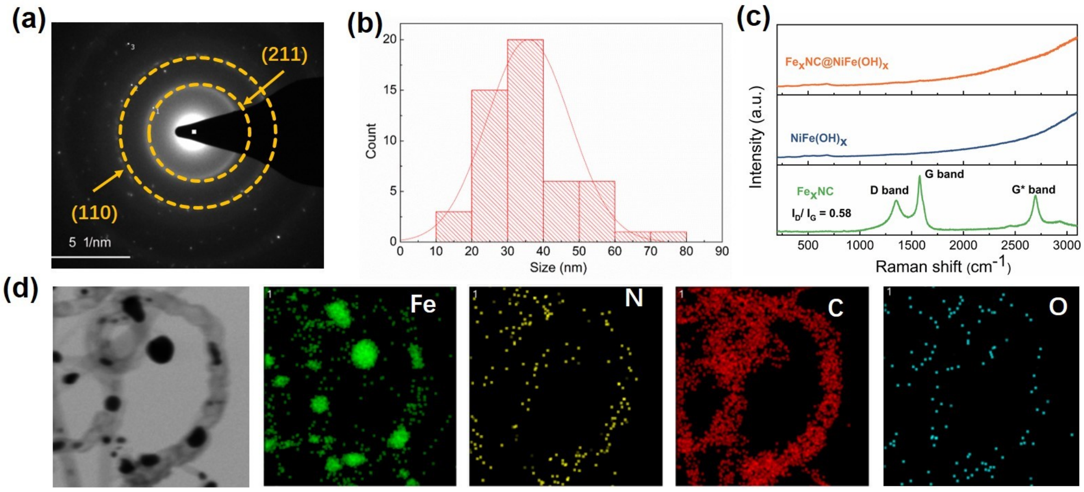

Fig. S2 (a) Fourier transform (FFT) image of Fe_xNC. (b) Size distribution of nanoparticles measured from Fig. 1d. (c) Raman spectra of as-prepared electrodes (d) Energy-dispersive X-ray spectroscopy (EDS) elemental mapping images of Fe_xNC.

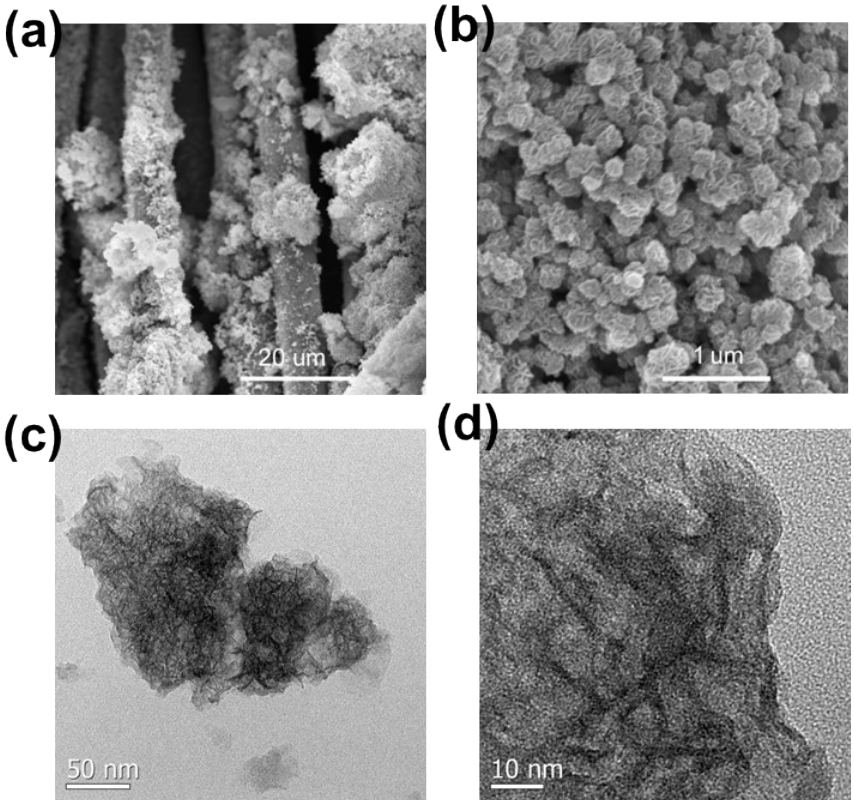

Fig. S3 (a, b) SEM images of $NiFe(OH)_x$ on carbon cloth and (c, d) TEM images of $NiFe(OH)_x$.

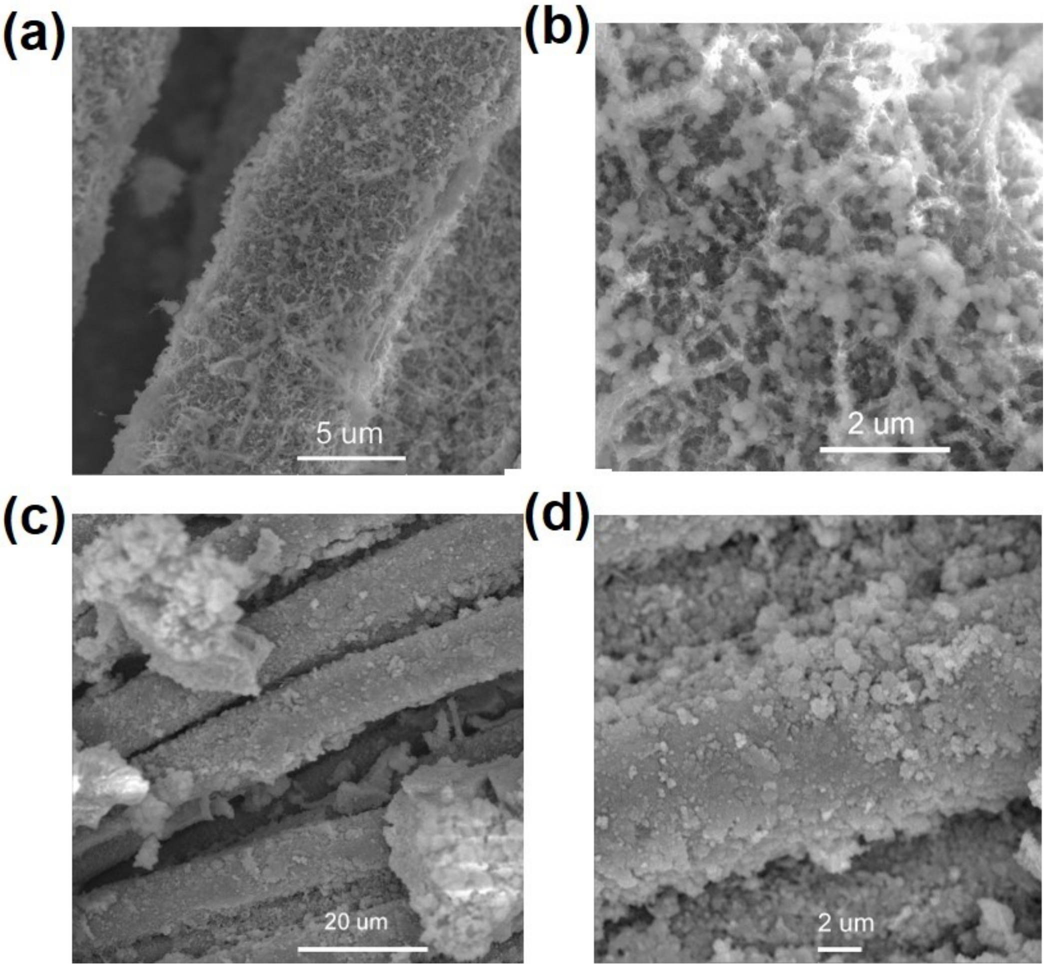

Fig. S4 SEM images of (a, b) $Fe_xNC@NiFe(OH)_x$-0.3 and (c, d) $Fe_xNC@NiFe(OH)_x$-10.

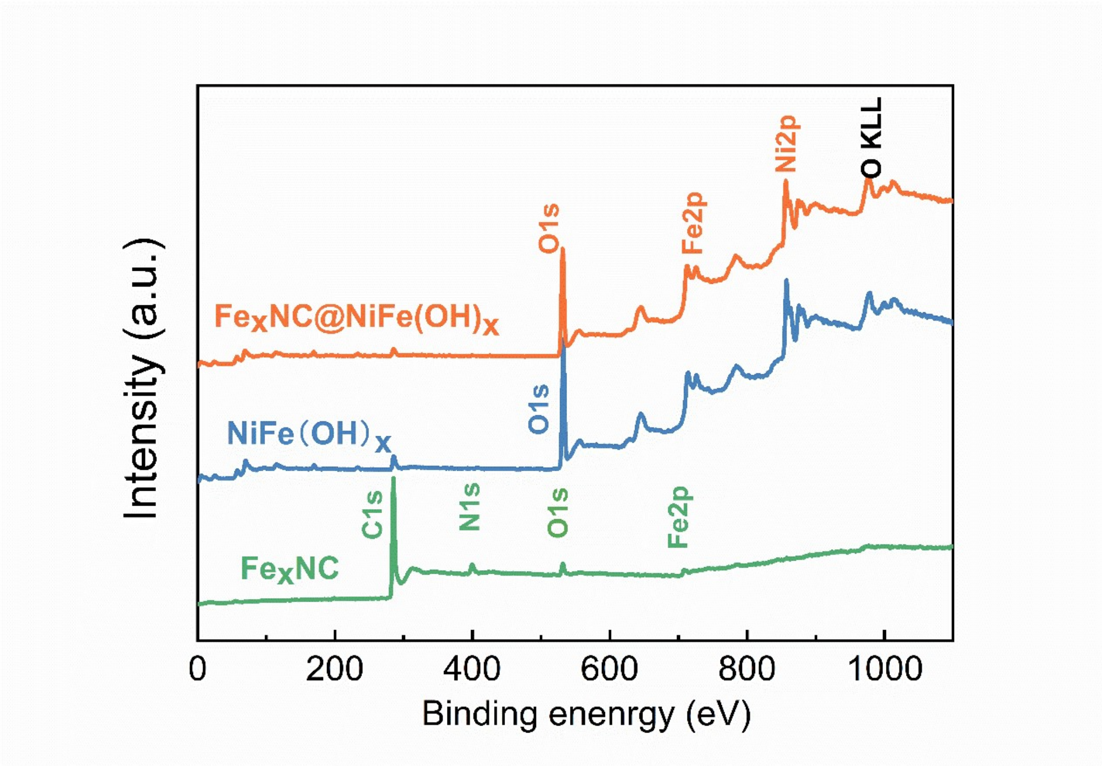

Fig. S5 Full XPS survey spectra of $Fe_xNC@NiFe(OH)_x$, $NiFe(OH)_x$ and Fe_xNC.

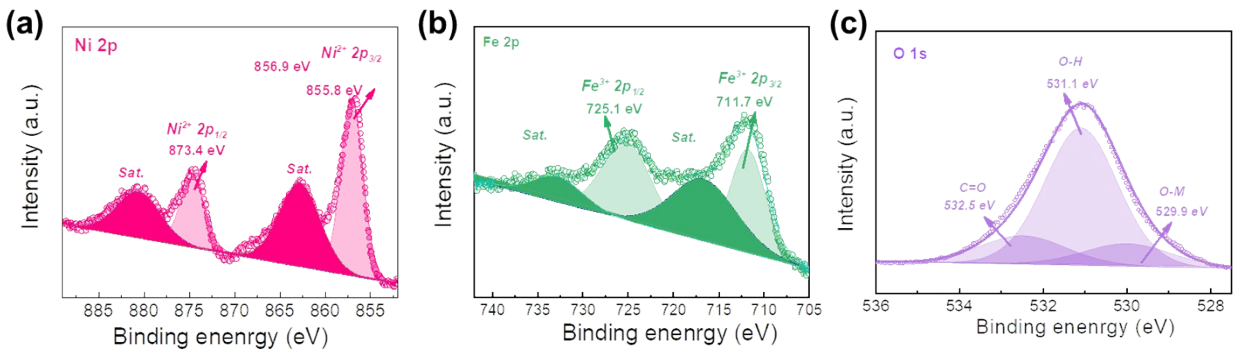

Fig. S6 High resolution XPS spectra of $NiFe(OH)_x$: (a) Ni 2p, (b) Fe 2p and (c) O 1s.

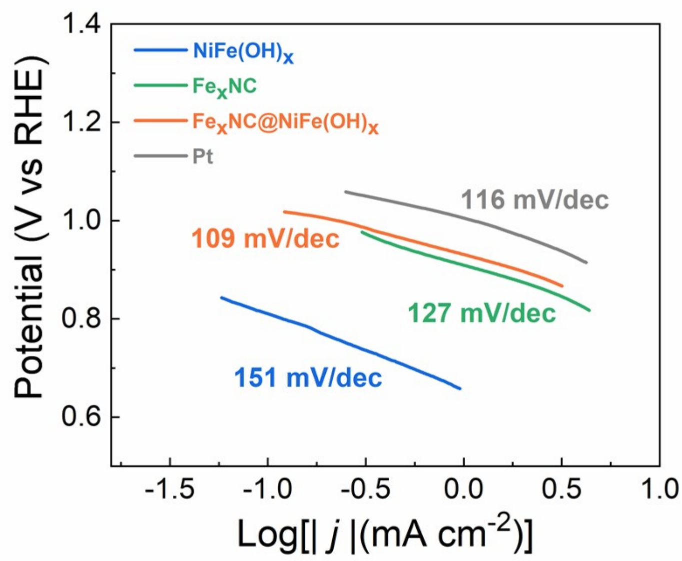

Fig. S7 ORR Tafel slopes of $Fe_xNC@NiFe(OH)_x$, $NiFe(OH)_x$, Fe_xNC and Pt.

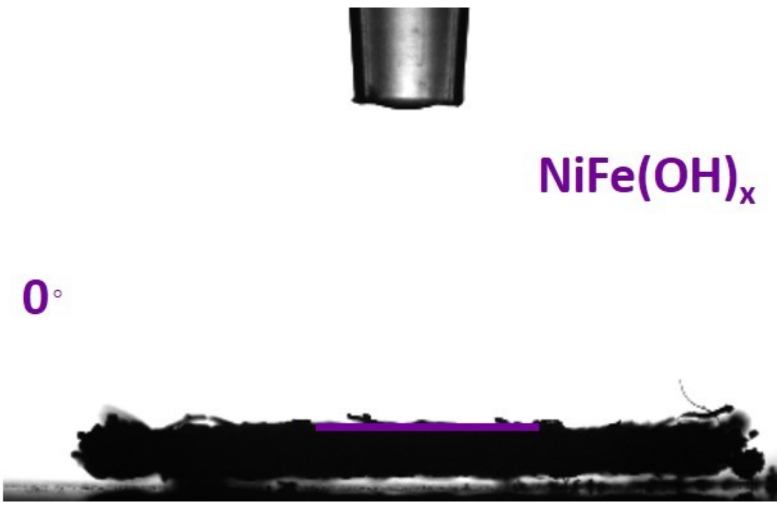

Fig. S8 Contact angle evaluation on $NiFe(OH)_x$.

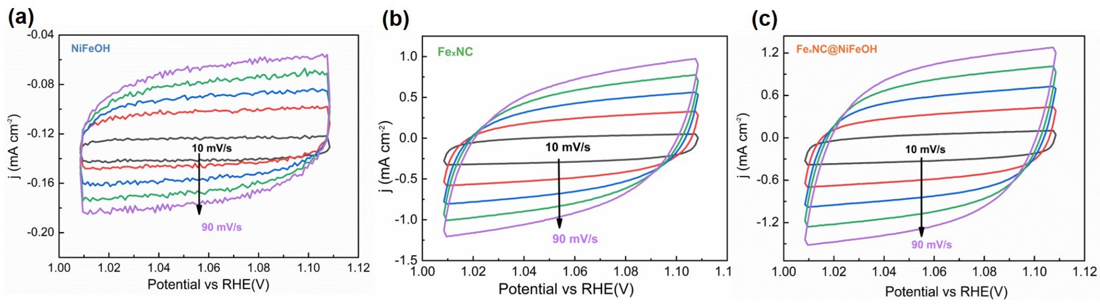

Fig. S9 The CV curves recorded between 1.00 V and 1.12 V at different scan rates on (a) $NiFe(OH)_x$, (b) Fe_xNC, and (c) $Fe_xNC@NiFe(OH)_x$.

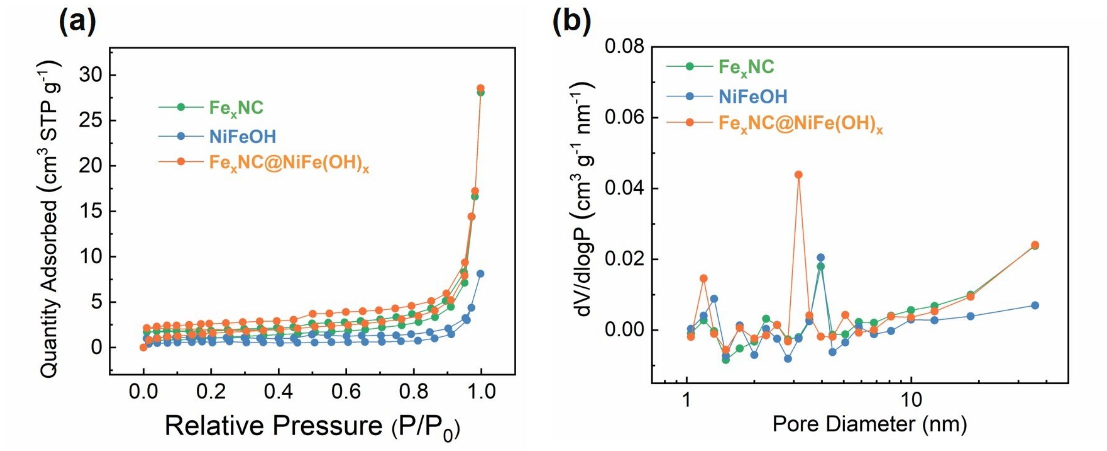

Fig. S10 (a) N_2 adsorption/desorption isotherms and (b) BJH pore size distribution of Fe_xNC, $NiFe(OH)_x$, and $Fe_xNC@NiFe(OH)_x$, respectively.

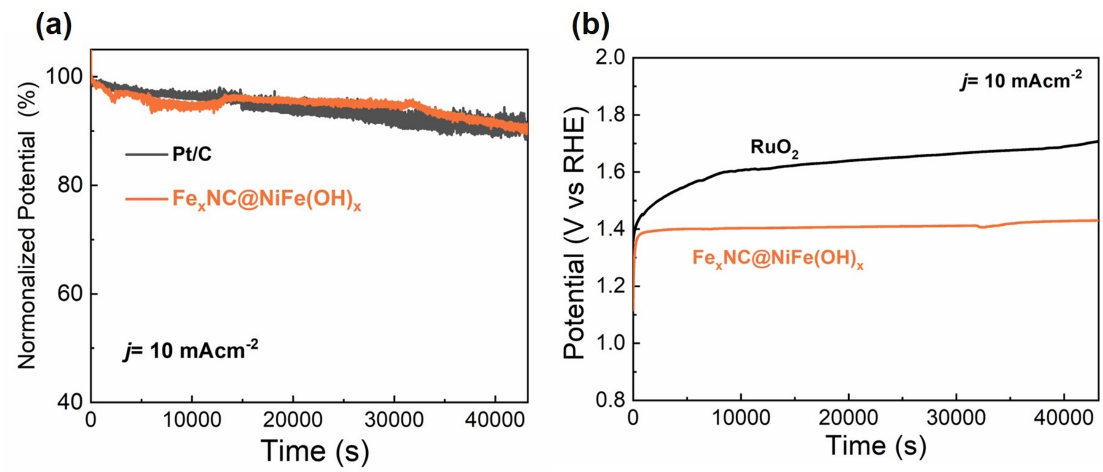

Fig. S11 (a) Chronopotentiometric test of Pt/C and $Fe_xNC@NiFe(OH)_x$ at 10 mA cm^{-2}**.** (b) Chronopotentiometry test of RuO_2 and $Fe_xNC@NiFe(OH)_x$ at 10 mA cm^{-2}**.**

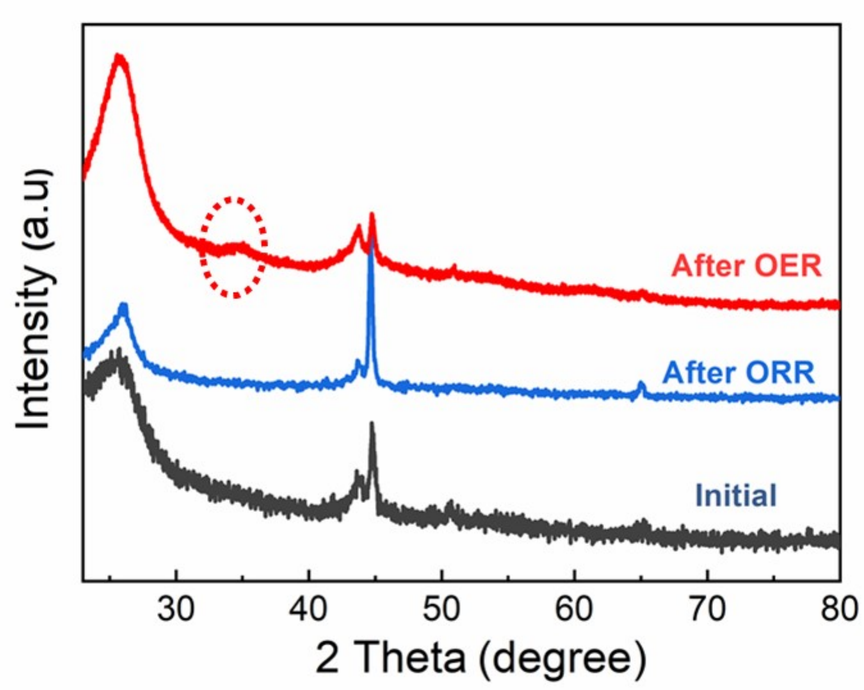

Fig. S12 XRD patterns of $Fe_xNC@NiFe(OH)_x$ electrode after 12 h OER and ORR.

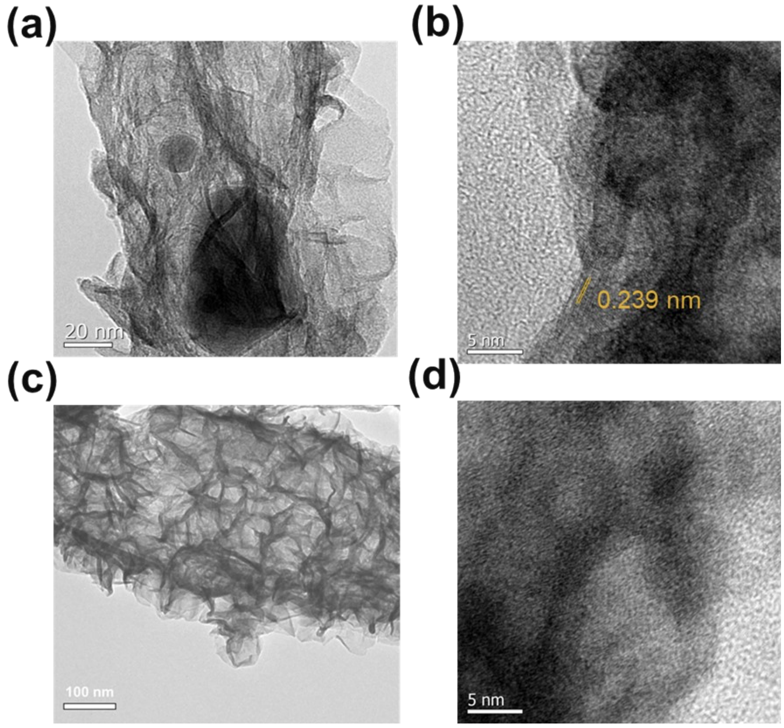

Fig. S13 TEM image of $Fe_xNC@NiFe(OH)_x$ after 12 h (a, b) OER and (c, d) ORR.

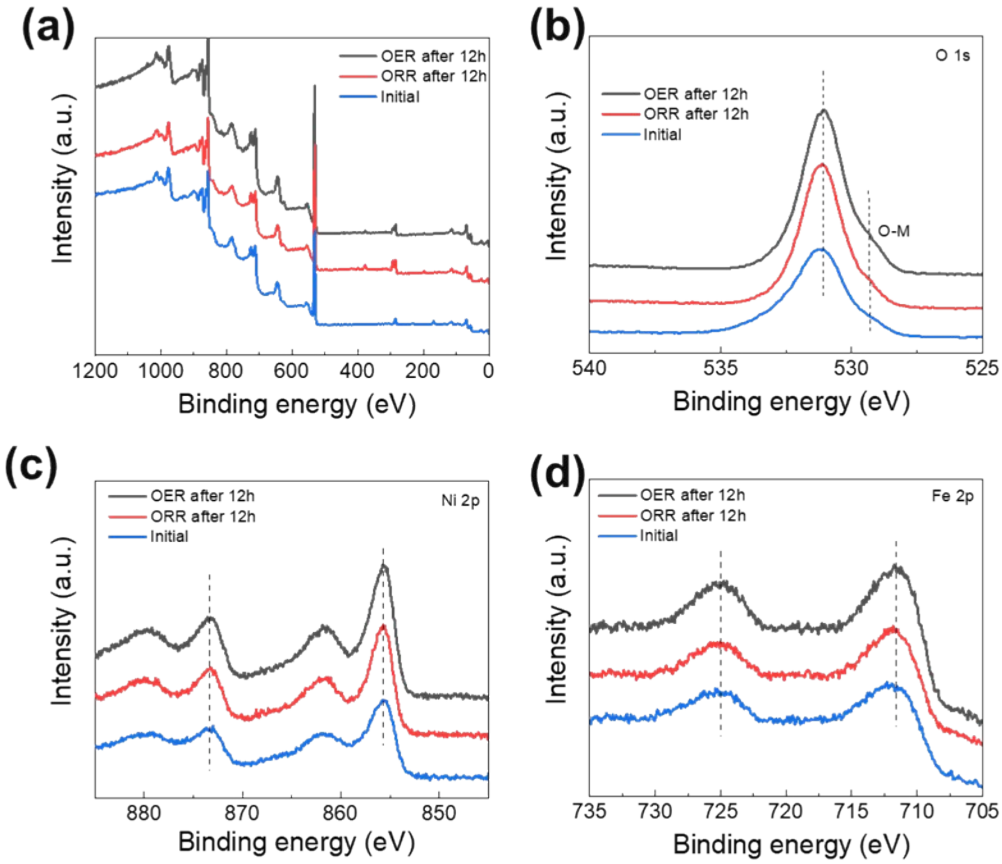

Fig. S14 XPS plots of post-OER electrode, post-ORR electrode and the initial one: (a) full survey spectra, (b) O 1s, (c) Ni 2p and (d) Fe 2p.

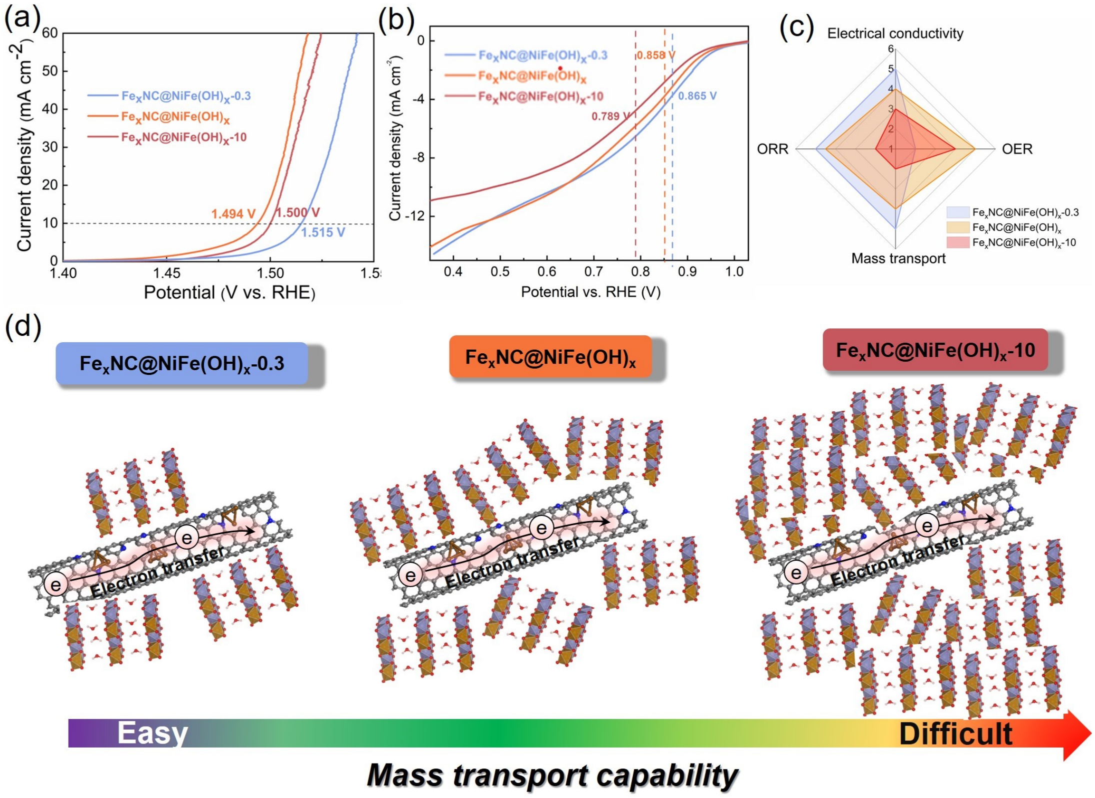

Fig. S15 Electrocatalytic performance of electrodes with different deposition times for (a) OER, (b) ORR and (c) comparison of their physicochemical characteristics. (d) Schematic illustration of mass transport capability on electrodes with different amounts of $NiFe(OH)_x$.

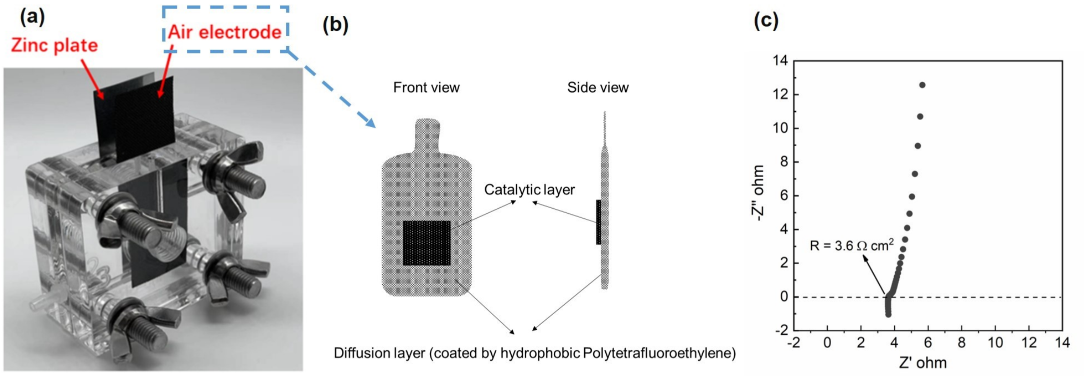

Fig. S16 (a) The photo of a homemade zinc-air battery. (b) The configuration of the air cathode. (c) Corresponding EIS of ZABs: the intersection of X-axis represents the electronic resistance in the cell.

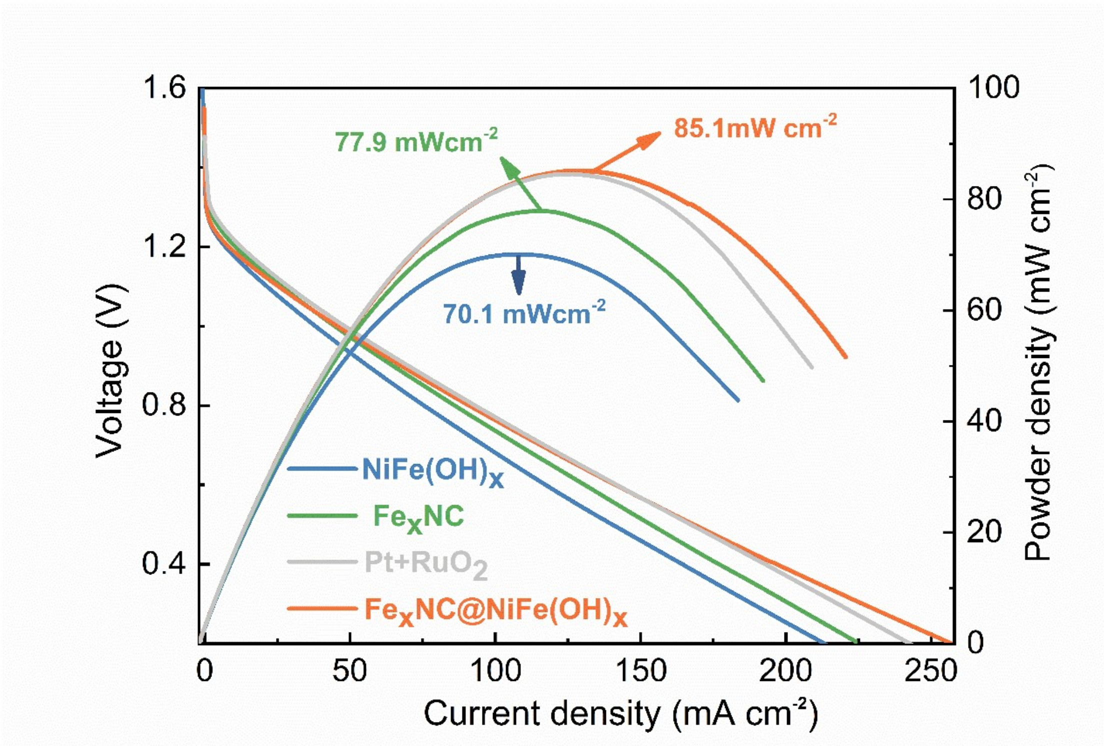

Fig. S17 The power density of ZABs with different electrodes.

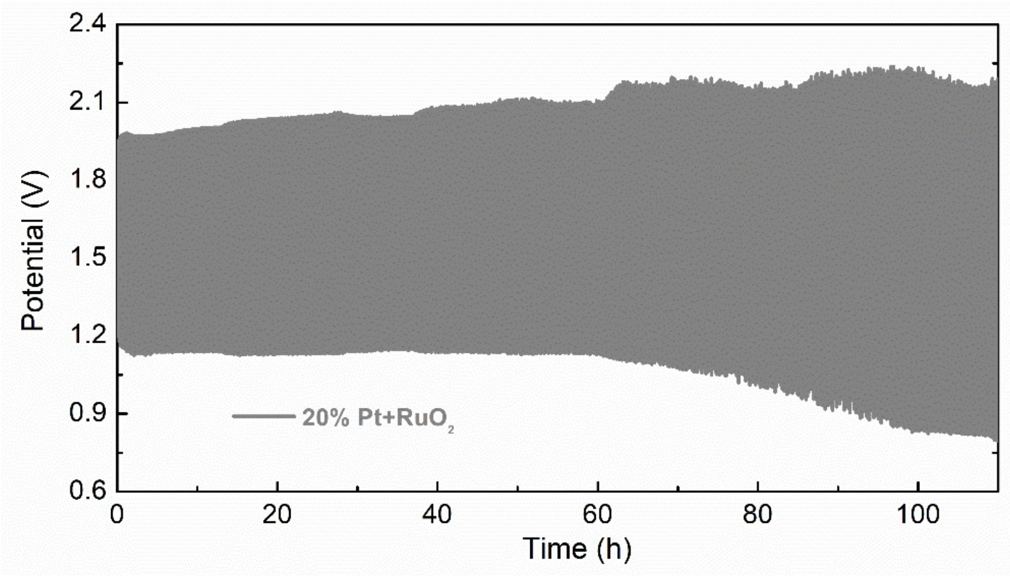

Fig. S18 The discharge/charge curves of Zn-air battery with electrode of 20 % Pt and RuO_2 at 10.0 mA cm^{-2}.

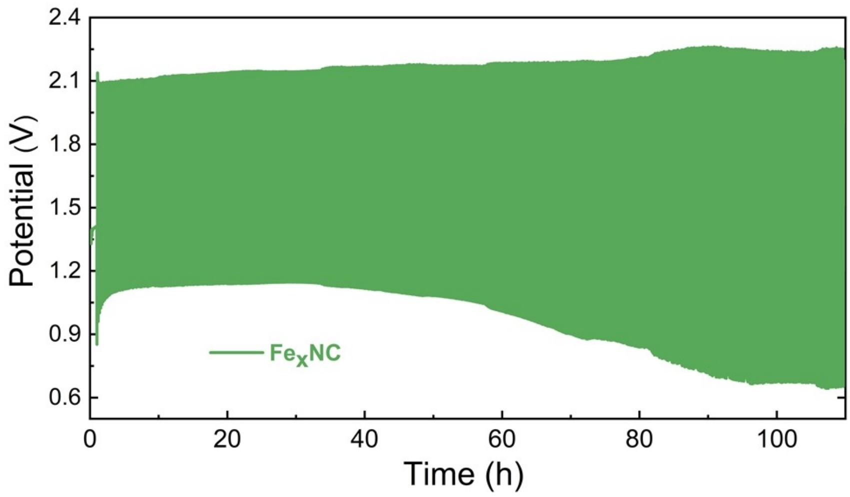

Fig. S19 The discharge/charge curves of Zn-air battery with electrode of Fe_xNC at 10.0 mA cm^{-2}.

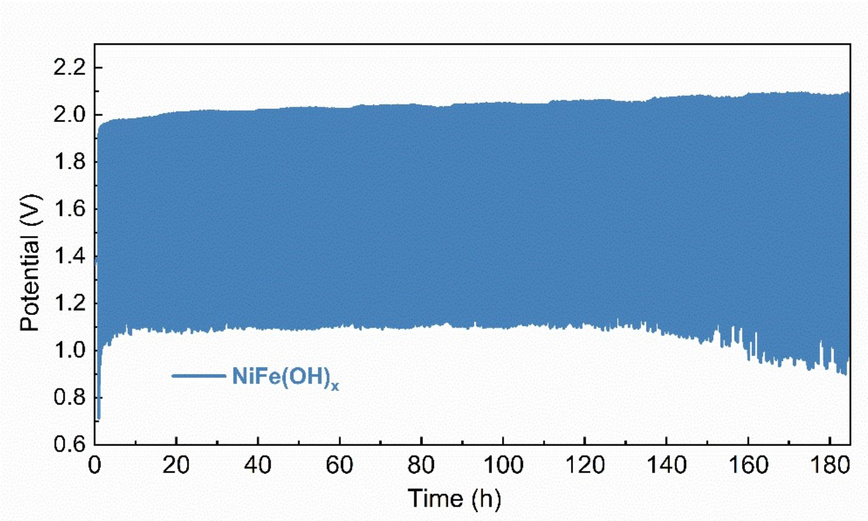

Fig. S20 The discharge/charge curves of Zn-air battery with electrode of $NiFe(OH)_x$ at 10.0 mA cm^{-2}.

Table S1 EDS results of the prepared electrodes (wt. %).

	Wt. %		
	FeNC	NiFe(OH)x	Fe_xNC@NiFe(OH)x
Fe	8.19	2.5	19.62
Ni	-	3.42	16.79
C	90.12	15.31	46.02
O	-	78.78	17.58
N	1.56	-	-

Table S2 Proportion of graphitic N, pyrrolic N, Fe-N_x and pyridinic N in the Fe_xNT according to the XPS analysis.

Types	Pyridine-N	Fe-N	Pyrolytic-N	Graphical-N	Oxidized -N
Contents	30.9%	20.3%	11.9%	22.1%	14.8%

Table S3 XPS results of the prepared electrodes (at. %).

	Atomic %		
	FeNC	NiFe(OH)x	Fe_xNC@NiFe(OH)x
Fe	0.89	12.19	14.09
Ni	-	16.18	16.98
C	92.17	17.17	11.18
O	-	53.25	57.13
N	0.09	-	-

Table S4 Comparison of $E_{j=10}$ and $E_{1/2}$ on different electrodes.

Catalysts	**$E_{j=10}$ (V)**	**$E_{1/2}$ (V)**
Fe_xNC@NiFe$(OH)_x$	1.494	0.858
Fe_xNC	1.607	0.825
NiFe$(OH)_x$	1.511	0.685
RuO_2/Pt/C	1.562	0.899

Table S5 BET surface area and pore volume of the different electrocatalysts.

Catalysts	**BET surface area (m^2 g^{-1})**	**Pore volume (cm^3 g^{-1})**
Fe_xNC	4.14	0.039
NiFe$(OH)_x$	2.54	0.011
Fe_xNC@NiFe$(OH)_x$	5.88	0.041

Table S6 Comparison of electrochemical performance on previously reported electrodes ZABs

Catalysts	η@10 mA (V)	E 1/2 (V)	Δ E (V)	Current density (mA cm^{-2})	Cycling hours (hrs)	Reference
$Fe_xNC@NiFe(OH)_x$	0.264	0.858	0.636	10	350	This work
Co_3O_4/WS_2	0.330	0.81	0.750	5	16	1
NiFe-LDH/Co,N-CNF	0.312	0.790	0.752	25	80	2
Co_3O_4@POF	0.33	0.82	0.74	10	60	3
Fe/N/C@BMZIF	0.41	0.85	0.79	10	17	4
Fe,Ni–N–C/N-CNT	0.315	0.879	0.666	10	200	5
$NiCo_2O_4$@NiCoFe–OH	0.235	0.77	0.695	10	250	6

Table S7 Comparison of ZAB performances with $Fe_xNC@NiFe(OH)_x$, $Pt/C+RuO_2$, and other reported cathodes operating at 10 mA cm^{-2}.

Electrodes	Voltage gap(V)	Cycle number	Reference
$Fe_xNC@NiFeOH$	0.81	2000	This work
$Pt/C+RuO_2$	0.87	530	This work
Zn-Co-S-NN/CFP	0.85	200	7
Cu-Foam@CuCoNC-500	0.8	1080	8
CMO/NCNF	0.93	350	9
NiS_x-FeO_y/SCFP	1.00	55	10
Fe-N/C-1/30	1.00	50	11
$NiCo_2O_4$@NiCoFe-OH	0.83	500	6
Co@NCNTA/CC	0.80	1020	12
am-Fe-Bi/NF	0.60	85	13
Co_3O_4@NiFe LDH	0.80	1200	14
N-Co/CNF	0.74	100	15
Co_4N/CNW/CC	0.84	408	16
NC-Co_3O_4/CC-600	0.87	106	17
CoO_x@NC	0.80	110	18
NCCo/CoN_x	0.80	1200	19
CMO–U@CC	0.70	150	20
NiFe/NCNF/CC	0.79	700	21

References:

1. Y. Ling, M. Li, K. Qu, Z. Yang, Electronically interacted Co_3O_4/WS_2 as superior oxygen electrode for rechargeable zinc-air batteries, *Chem. Commun.*, **2020**, *56*, 15193-15196.

2. Q. Wang, L. Shang, R. Shi, X. Zhang, Y. Zhao, G. I. N. Waterhouse, L. Z. Wu, C.H. Tung, T. Zhang, NiFe layered double hydroxide nanoparticles on Co, N-Codoped carbon nanoframes as efficient bifunctional catalysts for rechargeable Zinc-air batteries, *Adv. Energy Mater.,* **2017**, *7*, 1700467.

3. J. N. Liu, B. Q. Li, C. X. Zhao, J. Yu, Q. Zhang, A composite bifunctional oxygen electrocatalyst for high-performance rechargeable Zinc-air batteries, *ChemSusChem,* **2020,** *13*, 1529.

4. M. Wang, T. Qian, J. Zhou, C. Yan, An efficient bifunctional electrocatalyst for a zinc-air battery derived from Fe/N/C and bimetallic metal-organic framework composites, *ACS Appl. Mater. Interfaces,* **2017**, *9*, 5213-5221.

5 J. Fang, X. Zhang, X. Wang, D. Liu, Y. Xue, Z. Xu, Y. Zhang, C. Song, W. Zhu, Z. Zhuang, A metal and nitrogen doped carbon composite with both oxygen reduction and evolution active sites for rechargeable zinc-air batteries, *J. Mater. Chem. A,* **2020**, *8*, 15752.

6. S. Li, X. Yang, S. Yang, Q. Gao, S. Zhang, X. Yu, Y. Fang, S. Yang, X. Cai, An amorphous trimetallic (Ni-Co-Fe) hydroxide-sheathed 3D bifunctional electrode for superior oxygen evolution and high-performance cable-type flexible zinc-air batteries, *J. Mater. Chem. A,* **2020**, *8*, 5601-5611.

7. X. Wu, X. Han, X. Ma, W. Zhang, Y. Deng, C. Zhong, W. Hu, Morphology-controllable synthesis of Zn-Co-mixed sulfide nanostructures on carbon fiber paper toward efficient rechargeable zinc-air batteries and water electrolysis, *ACS Appl. Mater. Interfaces,* **2017**, *9*, 12574-12583.

8. H. Sun, Q. Li, Y. Lian, C. Zhang, P. Qi, Q. Mu, H. Jin, B. Zhang, M. Chen, Z. Deng, Y. Peng, Highly efficient water splitting driven by zinc-air batteries with a single catalyst incorporating rich active species, *Appl. Catal., B,* **2020**, *263*, 118139.

9. X. Chen, Z. Yan, M. Yu, H. Sun, F. Liu, Q. Zhang, F. Cheng, J. Chen, Spinel oxide nanoparticles embedded in nitrogen-doped carbon nanofibers as a robust and self-standing bifunctional oxygen cathode for Zn–air batteries, *J. Mater. Chem. A,* **2019**, *7*, 24868-24876.

10. Y. Cheng, D. Li, L. Shi, Z. Xiang, Efficient unitary oxygen electrode for air-based flow batteries, *Nano Energy* **2018**, *47*, 361-24876.

11. W. Wei, X. Shi, P. Gao, S. Wang, W. Hu, X. Zhao, Y. Ni, X. Xu, Y. Xu, W. Yan, H. Ji, M. Cao, Well-elaborated mechanochemically synthesized Fe-TPP⊂ZIF precursors (Fe-TPP = tetraphenylporphine iron) to atomically dispersed iron–nitrogen species for oxygen reduction reaction and Zn-air batteries, *Nano Energy* **2018**, *52*, 29-37.

12. L. Liu, Y. Wang, F. Yan, C. Zhu, B. Geng, Y. Chen, S. l. Chou, Cobalt-encapsulated nitrogen-doped carbon nanotube arrays for flexible zinc-air batteries, *Small Methods* **2020**, *4*, 1900571.

13. W. Zhao, T. Xu, T. Li, Y. Wang, H. Liu, J. Feng, S. Ding, Z. Li, M. Wu, Amorphous Iron (III)-borate nanolattices as multifunctional electrodes for self-driven overall water splitting and rechargeable Zinc-air battery, *Small* **2018**, *14*, 1802829.

14. X. Guo, X. Hu, D. Wu, C. Jing, W. Liu, Z. Ren, Q. Zhao, X. Jiang, C. Xu, Y. Zhang, N. Hu, Tuning the bifunctional oxygen electrocatalytic properties of core–shell Co_3O_4@NiFe LDH Catalysts for Zn-air batteries: effects of interfacial cation valences, *ACS Appl. Mater. Interfaces.* **2019**, *11*, 21506-21514.

15. P. Rao, P. Cui, Z. Wei, M. Wang, J. Ma, Y. Wang, X. Zhao, Integrated N-Co/carbon nanofiber cathode for highly efficient zinc-air batteries, *ACS Appl. Mater. Interfaces* **2019**, *11*, 29708-29717.

16. F. Meng, H. Zhong, D. Bao, J. Yan, X. Zhang, In situ coupling of strung Co_4N and intertwined N-C fibers toward free-standing bifunctional cathode for robust, efficient, and flexible Zn-air batteries, *J. Am. Chem. Soc.,* **2016**, *138*, 10226-10231.

17. Q. Liu, L. Wang, X. Liu, P. Yu, C. Tian, H. Fu, N-doped carbon-coated Co_3O_4 nanosheet array/carbon cloth for stable rechargeable Zn-air batteries, *Sci. China Mater.,* **2018**, *62*, 624.

18. Y. Hao, Y. Xu, N. Han, J. Liu, X. Sun*,* Boosting the bifunctional electrocatalytic oxygen activities of CoO_x nanoarrays with a porous N-doped carbon coating and their application in Zn-air batteries*, J. Mater. Chem. A,* **2017***, 5,* 17804-17810.

19. C. Guan, A. Sumboja, W. Zang, Y. Qian, H. Zhang, X. Liu, Z. Liu, D. Zhao, S. J. Pennycook, J. Wang*,* Decorating Co/CoN_x nanoparticles in nitrogen-doped carbon nanoarrays for flexible and rechargeable zinc-air batteries, *Energy Storage Mater.,* **2019***, 16,* 243-250.

20. J. Qian, X. Guo, T. Wang, P. Liu, H. Zhang, D. Gao, Bifunctional porous Co-doped NiO nanoflowers electrocatalysts for rechargeable zinc-air batteries, *Appl. Catal. B,* **2019**, *250*, 71-77.

21. C. Lai, J. Fang, X. Liu, M. Gong, T. Zhao, T. Shen, K. Wang, K. Jiang, D. Wang, In situ coupling of NiFe nanoparticles with N-doped carbon nanofibers for Zn-air batteries driven water splitting, *Appl. Catal. B,* **2021**, *285*,119856